

FAST PHOTODETECTOR BUNCH DURATION MONITOR FOR THE ADVANCED PHOTON SOURCE PARTICLE ACCUMULATOR RING*

J. Dooling[†], J. Calvey, K. Harkay, C. Y. Yao, B. X. Yang, Argonne National Laboratory, Argonne, USA

Abstract

A fast photodetector system is used to monitor the bunch duration in the Advanced Photon Source (APS) Particle Accumulator Ring (PAR). The PAR Bunch Duration Monitor (BDM) is based on the metal-semiconductor-metal (MSM) photodetector Hamamatsu G4176-03 MSM with specified rise and fall times of 30 ps. The BDM has sufficient frequency response to resolve the PAR bunch near extraction where, under low-charge conditions, minimum rms pulse durations of 250-300 ps are observed. Beam from the PAR is injected into the Booster; for efficient capture, injected rms bunch duration from the PAR must be less than 650 ps. BDM data show good agreement with streak camera measurements. The MSM detector exhibits a ringing response to fast input signals. To overcome this, the BDM output is de-convolved with the impulse response function of the detector-amplifier circuit. Turn-by-turn bunch duration data is presented versus charge and time in the PAR cycle. Peak detection mode allows for calculation of bunch length over large fractions of the PAR cycle.

INTRODUCTION

A fast metal-semiconductor-metal (MSM) photodetector is used to detect synchrotron light from the APS particle accumulator ring (PAR). The MSM detector and amplifier electronics form the PAR bunch duration monitor (BDM). However, direct measurements from the BDM show distorted waveforms as shown in Figure 1a. The reconstructed waveform of the same pulse is presented in Fig. 1b and is generated by deconvolution processing. Here we describe a method to determine the bunch length from a deconvolution of the observed waveform and impulse response function for the detector and amplifier. The impulse response waveform is measured using second harmonic (SH, $\lambda=527$ nm) light produced by the APS PC Gun drive laser. Measurements [1] indicate the SH laser pulse duration to be 6-7 ps FWHM ($\sigma_t \sim 2.5$ -3.0 ps). The design of the optical synchrotron radiation collection system has been previously described [2, 3].

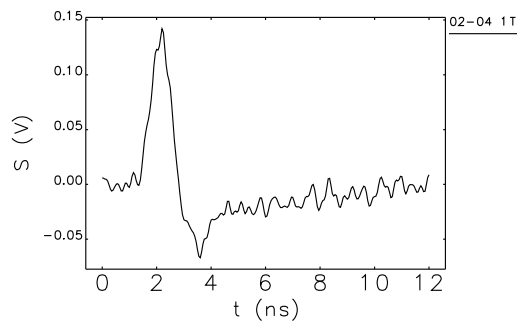
The convolution integral may be expressed as,

$$y(t) = \int_0^t f(\lambda)h(t-\lambda)d\lambda \approx \sum_{i=0}^{\infty} (f(i\Delta T)\Delta T) h(t-i\Delta T), \quad (1)$$

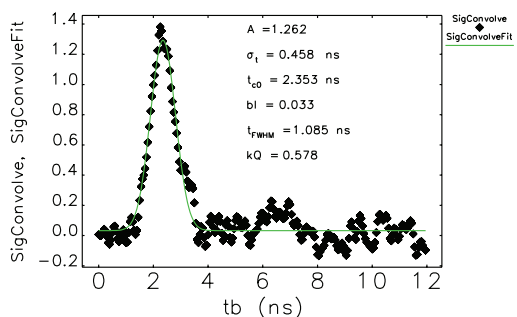
where $y(t)$ is the observed waveform, $f(\lambda)$ is the input signal, $h(t)$ is the circuit impulse response function, and

* Work supported by the U.S. Department of Energy, Office of Science, Office of Basic Energy Sciences, under Contract No. DE-AC02-06CH11357.

[†] jcdooling@anl.gov



(a) BDM raw signal.



(b) Deconvolved waveform with Gaussian fit.

Figure 1: Raw and processed BDM data; 914 ms, 5.6 nC.

$\lambda = i\Delta T$. In the frequency domain, Eq. 1 can be written simply as the product of the Fourier transforms of each time domain function,

$$Y(\omega) = F(\omega)H(\omega) \quad (2)$$

$$F(\omega) = \frac{Y(\omega)}{H(\omega)} \rightarrow \mathcal{F}^{-1}(F(\omega)) = f(t) \quad (3)$$

The visible-wavelength synchrotron light intensity is proportional to the instantaneous current in the pulse and therefore is the bunch waveform we wish to determine, $f(t)$. Since the observed waveform, $y(t)$ is the convolution of $f(t)$ and $h(t)$, the inverse deconvolution operation must be performed. Deconvolution is carried out using `sddsconvolve` with the `-deconvolve` option [4]. Deconvolution requires division in the frequency domain which adds noise to the deconvolved waveform; prior to fitting, the deconvolved waveforms are smoothed using `sddssmooth` [5].

MEASUREMENTS

Impulse Response

The photodetector is a Hamamatsu MSM G4176-03, SMA-mounted device with rise and fall times both given as 30 ps. [6]. The detector is mounted on a bias tee fol-

Content from this work may be used under the terms of the CC BY 3.0 licence (© 2018). Any distribution of this work must maintain attribution to the author(s), title of the work, publisher, and DOI.

followed by two HD Communications Corp. HD27066 broadband amplifiers [7], each providing 21 dB of gain at 4 GHz; Figure 2 shows the layout schematically. Element values

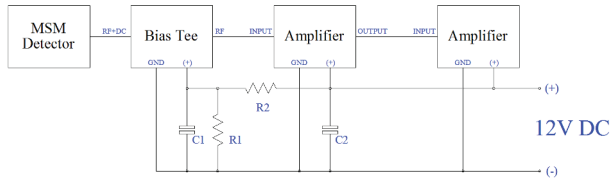


Figure 2: MSM photodetector amplifier schematic.

for the circuit are as follows: $R1=50\text{ k}\Omega$, $R2=15\text{ k}\Omega$, and $C1=C2=10\text{ nF}$. The resistors act as a voltage divider to provide 9 V though the bias tee to the MSM.

The photodetector peak power specification is 50 mW for pulse durations less than 1 ns; to meet this requirement with the PC Gun drive laser pulse, diffuse reflection from inner wall of the laser transport enclosure was employed to provide attenuation. The attenuation factor α_d is approximately the product of the wall reflectivity, R and the ratio of the detector area to the area of a hemisphere whose radius is defined as the distance from the laser spot to the detector.

$$\alpha_d = R \frac{A_d}{A_h} = R \frac{A_d}{2\pi r_d^2}, \quad (4)$$

where A_d is the detector area (0.04 mm^2) and r_d is the laser spot-detector separation (165 mm). Assuming a reflectivity of 0.5, $\alpha_d = 1.2 \times 10^{-7}$. The SH rms pulse duration is 2.5 ps or 5.9 ps, FWHM [1]. The peak SH power may be expressed approximately as, $P_{SH} \approx E_{SH}/\tau_{FWHM}$. A laser energy of $2\text{ }\mu\text{J}$ was chosen to generate the impulse response measurement. For $E_{SH} = 2\text{ }\mu\text{J}$, $P_{SH} = 340\text{ kW}$ and the power on detector, $P_d = \alpha_d P_{SH} = 40\text{ mW}$. The laser pulse is short enough to be regarded as a delta function for the detector-amplifier circuit.

Measured impulse responses at $2\text{ }\mu\text{J}$ are presented in Figure 3; which represents the average of 3 separate laser impulse waveforms. The waveforms are sampled at a rate of 20 GS/s. Gaussian fits to the main pulse yield an average rms duration of 60.5 ps and show roughly 34 ps of rms jitter in terms pulse centroid. The jitter is a significant fraction of the impulse response duration. To remove the jitter component, the average impulse response is obtained by 1) oversampling the waveform data at 1 TS/s, 2) correcting the waveforms to the nearest ps for centroid differences determined from the Gaussian fits, 3) averaging the adjusted waveforms, and 4) resampling the average at 20 GS/s. The resultant impulse response waveform is shown in Figure 3. Though most has been subtracted out, the noise prior to the main pulse appears to come partly from HV switching on the laser Pockels Cell. The total duration of the impulse response waveform is 12 ns or 240 samples. The time span is sufficient to allow us to look for double-bunching after the 12th-harmonic rf is introduced.

Figure 1a shows the initial raw signal pulse in a BDM data set comprising 128 turns ($13.1\text{ }\mu\text{s}$) for a bunch charge

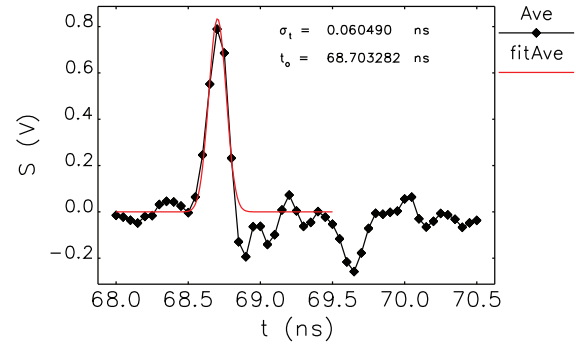


Figure 3: Average Impulse Response Waveform

of 5.6 nC near the end of the PAR cycle. In this case, the PAR is operating in 1-Hz mode where $t=0$ represents the initial injection of charge from the linac. The data in Fig. 1 are collected at $t=914\text{ ms}$; bunch extraction occurs near $t=980\text{ ms}$. The 12th-harmonic rf is introduced at $t=750\text{ ms}$ and serves to compress the bunch. The deconvolved waveform for this turn is presented in Figure 1b.

Bunch Duration with Charge

Charge from the 2856-MHz, s-band linac is injected into the PAR in a 10-ns macropulse at energies of 325, 375, or 425 MeV. The charge per linac macropulse is typically 1.0-1.2 nC and occurs at a rep rate of 30 Hz; therefore, 18-20 linac macropulses are required to store 20 nC. Injection to 20 nC then lasts between 567 and 633 ms leaving just over 100 ms for damping prior to introduction of the 12th harmonic rf.

BDM results versus accumulated charge at $t=914\text{ ms}$ are compared with streak camera (SC) measurements collected during the same October 9, 2017 study period in Figure 4. A later set of BDM measurements were made without SC data on November 13, 2017 after steps were taken to stabilize the beam at high charge; these data are also presented in Fig. 4. The BDM systematically indicates shorter bunch

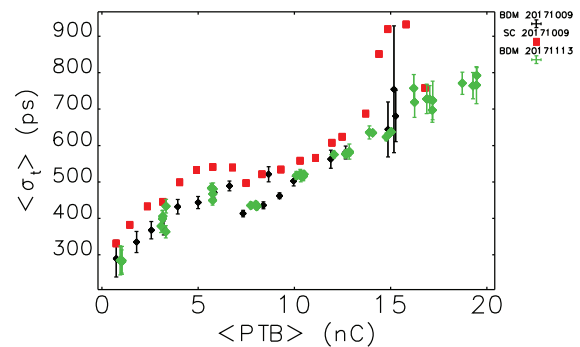


Figure 4: Comparison of BDM and Streak Camera RMS bunch duration with accumulated charge.

length than does the SC; however, the SC data is collected over a much longer period than the BDM, in this case: 5 ms vs. $13\text{ }\mu\text{s}$. Averaging will tend to smear out the SC

bunch distribution, increasing the bunch length. Good reproducibility is observed in the BDM data for the two different dates; error bars represent the standard deviation of the turn-by-turn (TBT) σ_t data for all 128 turns. The results presented in Fig. 4 are consistent with SC measurements given in Fig. 6 of Ref. [8]. Fluctuations in bunch length at low charge are the result of noise at low signal levels; at high charge, length variations are due to instabilities and oscillations in the bunch.

Longitudinal oscillations such as breathing mode are evident in higher-charge BDM data. Examples of this mode are given in Figure 5 from two separate PAR cycles, both with 15 nC of accumulated charge; single sinusoidal fits are also presented showing 3/2 ratio in frequencies. The breathing mode is a coherent rotation of the bunch at harmonics of the synchrotron frequency, f_s . The oscillations presented in

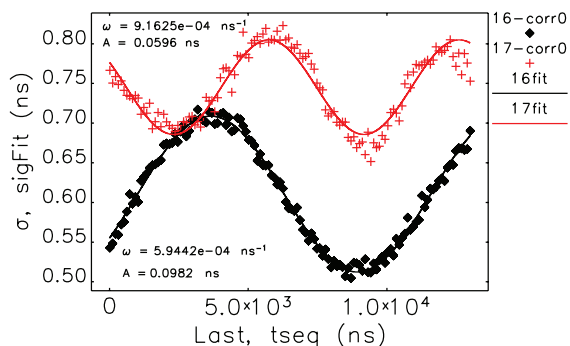


Figure 5: Self-excited bunch length modulation near the 2nd and 3rd harmonics of the synchrotron frequency along with sinusoidal fits.

Fig. 5 are self-excited. At the second harmonic, the bunch rotates through a time of longer duration and lower energy spread, followed a quarter-period later, $(4f_s)^{-1}$ by shorter length and higher energy spread. The additional energy spread may help to combat the growth of instabilities via Landau damping. Also, the breathing mode may provide a dynamic method to control the bunch length. At the highest charge, the BDM revealed large-scale filamentation of the bunch. Figure 6 provides contour plots of the longitudinal bunch profiles for charges of 5 and 13 nC. These data cover 128 turns or 13.1 μ s and are acquired near the end of the PAR cycle. Fig. 6b shows a dramatic increase in bunch length over what is observed at lower charge (Fig. 6a).

Peak Detect Mode

Data have also been collected in peak-detect mode, where the bunch length is derived from beam charge and pulse amplitude. Though detailed information about the longitudinal bunch profile is lost, the average duration can be calculated. In Figure 7, bunch duration versus time in the PAR cycle is presented for a range of bunch charge. The period extends from 0.6 to 1.0 second covering both the 12th-harmonic rf and extraction. Zooming in on the 9-nC case, prior to 12th harmonic, the inset shows a beating length modulation near 50 kHz. For these peak detect waveforms, 500 kS of data

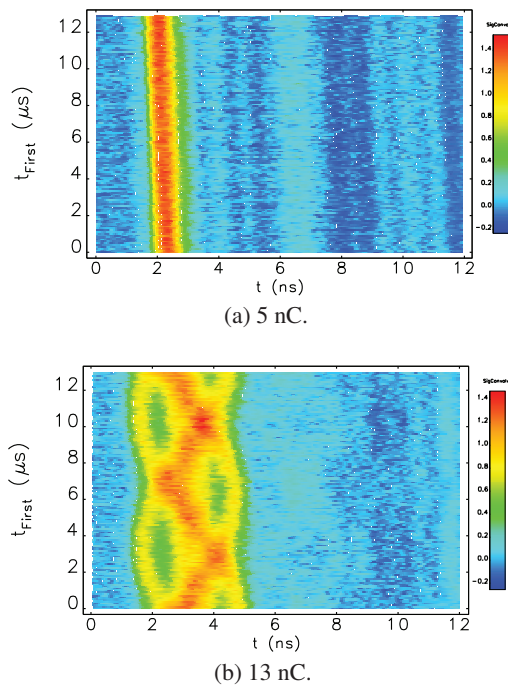


Figure 6: BDM contour plots over 128 turns (13.1 μ s) near 914 ms, 5 and 13 nC. Note the appearance of charge islands rotating in time (phase) for the 13-nC case.

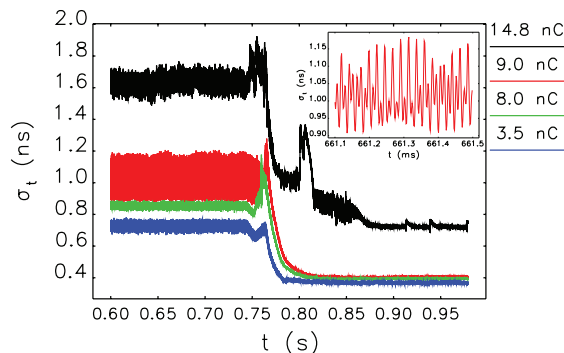


Figure 7: Peak detect bunch length measurements at 3.5, 8.0, 9.0, and 14.8 nC during the last 400 ms of the PAR cycle. Inset zooms in on oscillations for the 9-nC cycle prior to 12th harmonic.

are collected at a 1.25 MS/s rate.

SUMMARY

Good agreement is seen between PAR bunch length measured with the the BDM and streak camera. The BDM has revealed large pulse duration growth at high-charge, the mechanisms and mitigations for which are now under active investigation. An oscilloscope with deeper memory has been installed to allow us to follow TBT data for longer periods and observe transitions into and out of various oscillations.

ACKNOWLEDGMENT

Thanks to H. Shang, R. Soliday, and P. Dombrowski.

REFERENCES

- [1] J. C. Dooling and A. H. Lumpkin, "Streak Camera Measurements of the APS PC Gun Drive Laser," in Proc. NAPAC'16, Chicago, US, October 2016, paper MOPOB08, pp.85-88.
- [2] A.H. Lumpkin and B. X. Yang, "Status of the Synchrotron Radiation Monitors for the APS Facility Rings," in Proc. PAC 1995, Dallas, 2470-2472.
- [3] W. Berg, B. Yang, A. Lumpkin, and J. Jones, "Design and commissioning of the photon monitors and optical transport lines for the advanced photon source positron accumulator ring," AIP Conf. Proc. **390**, 483 (1997).
- [4] M. Borland, <https://ops.aps.anl.gov/manuals/SDDStoolkit/SDDStoolkitsu29.html\#x35-520004.22>
- [5] M. Borland, <https://ops.aps.anl.gov/manuals/SDDStoolkit/SDDStoolkitsu84.html\#x90-1070004.77>
- [6] <http://www.hamamatsu.com/resources/pdf/lsr/G4176E.pdf>
- [7] <http://www.rfcomp.com/download/HD27066specs.pdf>
- [8] C.-Y. Yao et al., "Beam Loading Measurement and its Application to the Harmonic RF Control of the APS PAR," Proc. EPAC 2006, Edinburgh, Scotland, 2006, p. 3538.